White Rose Research Online

eprints@whiterose.ac.uk
https://eprints.whiterose.ac.uk
Universities of Leeds, Sheffield and York

Deposited via The University of Leeds.

White Rose Research Online URL for this paper:
https://eprints.whiterose.ac.uk/id/eprint/112934/

Version: Accepted Version

Article:
Zhang, Y, Nahil, MA, Wu, C et al. (2017) Pyrolysis-catalysis of waste plastic using a nickel-stainless steel mesh catalyst for high value carbon products. Environmental Technology, 38 (22). pp. 2889-2897. ISSN: 0959-3330

https://doi.org/10.1080/09593330.2017.1281351

© 2017 Informa UK Limited, trading as Taylor & Francis Group. This is an Accepted Manuscript of an article published by Taylor & Francis in Environmental Technology on 11 Jan 2017, available online: http://dx.doi.org/10.1080/09593330.2017.1281351

Reuse
Items deposited in White Rose Research Online are protected by copyright, with all rights reserved unless indicated otherwise. They may be downloaded and/or printed for private study, or other acts as permitted by national copyright laws. The publisher or other rights holders may allow further reproduction and re-use of the full text version. This is indicated by the licence information on the White Rose Research Online record for the item.

Takedown
If you consider content in White Rose Research Online to be in breach of UK law, please notify us by emailing eprints@whiterose.ac.uk including the URL of the record and the reason for the withdrawal request.

UNIVERSITY OF LEEDS
University of Sheffield
UNIVERSITY of York

Pyrolysis-catalysis of waste plastic using a nickel-stainless steel mesh catalyst for high value carbon products

Yeshui Zhang [a], Mohamad A. Nahil [a], Chunfei Wu [b], Paul T. Williams [a*]

[a] School of Chemical & Process Engineering, University of Leeds, Leeds, LS2 9JT, UK

[b] Department of Chemical Engineering, University of Hull, Hull, HU6 7RX, UK

[*](Contact: Paul T. Williams: Email: p.t.williams@leeds.ac.uk)

ABSTRACT

A stainless steel mesh loaded with nickel catalyst was produced and used for the pyrolysis-catalysis of waste high density polyethylene with the aim of producing high value carbon products, including carbon nanotubes. The catalysis temperature and plastic to catalyst ratio were investigated to determine the influence on the formation of different types of carbon deposited on the nickel-stainless steel mesh catalyst. Increasing temperature from 700 to 900 °C resulted in an increase in the carbon deposited on the nickel loaded stainless steel mesh catalyst from 32.5 wt.% to 38.0 wt.%. The increase of sample to catalyst ratio reduced the amount of carbon deposited on the mesh catalyst in terms of g carbon g^{-1} plastic. The carbons were found to be largely composed of filamentous carbons, with negligible disordered (amorphous) carbons. Transmission electron microscopy analysis of the filamentous carbons revealed them to be composed of a large proportion (estimated at ~40%) multi-walled carbon nanotubes. The optimum process conditions for carbon nanotube production, in terms of yield and graphitic nature, determined by Raman spectroscopy, was catalysis temperature of 800 °C and plastic to catalyst ratio of 1:2 where a mass of 334 mg of filamentous/multi-walled carbon nanotubes g^{-1} plastic was produced.

Key words: Polyethylene; Pyrolysis; Carbon nanotubes; Catalysis; Waste

1. Introduction

There is current interest in carbon nanotubes as advanced materials due to their reported unique and advantageous properties in a range of industrial sectors such as electronics [1], biosensors [2], energy storage, reinforced composites etc. [3]. Carbon nanotubes are cylindrical hollow tubes composed of carbon with nano-sized diameters (0.1-100 nm) and long length (100m>). The nanotubes may be single-walled or multi-walled. Carbon nanotubes are most monnly produced by chemical vapour deposition [4]. The process involves high carbon content feedstocks such as methane, ethylene, benzene, xylenes, acetylene which interact with catalysts and form carbon nanotubes which grow on the catalyst surface [5, 6, 7, 8]. The process conditions range from 700 – 1200 °C and typical catalysts include Fe, Co, Ni, nano-particles and organometallic catalysts such as ferrocene, cobaltocene, nickelocene [9, 10, 11].

Waste plastics have been proposed as a feedstock to produce carbon nanotubes since when the plastics are subjected to pyrolysis, the polymer thermally degrades to produce a wide range of hydrocarbon gases. The carbon rich hydrocarbons can be regarded as suitable feedstock for the formation of carbon nanotubes by interaction with a suitable catalyst [12, 13, 14, 15, 16, 17]. Barzagan and McKay [13] have recently reviewed the production of carbon nanotubes from the thermal/catalytic processing of waste plastics. Kukovitskii et al [14] pyrolysed polyethylene in the presence of a nickel plate catalyst at 420-450 °C with the aim of producing carbon nanotubes, but the carbons were of poor quality. Yen et al [15] pyrolysed polyethylene in a fluidised bed reactor followed by a catalytic reactor at 700-800 °C with a Fe-MgO catalyst to produce carbon nanotubes. The authors have previously [12] used a pyrolysis-catalytic, two-reactor system to produce carbon nanotubes with a Ni-Ca-Al or Ni-Zn-Al catalyst using polypropylene as the feedstock. Later work using the same reactor system used real-world waste plastics derived from different industrial sources using a Ni-MN-Al catalyst

to produce carbon nanotubes, where contamination of the plastic with polyvinyl chloride led to distortion of the CNTs produced [17]. Liu et al [16] used a two-stage pyrolysis-catalyst reactor system to produce carbon nanotubes from polypropylene, the plastic was co-pyrolysed with zeolite to crack the plastic pyrolysis gases and the carbon nanotubes were produced in a second stage catalytic reactor using NiO catalyst. The optimum temperature for carbon nanotubes formation was 700 °C and 37 wt.% of carbon nanotubes were produced. A mixture of polyethylene and polypropylene was pyrolysed in a fluidised bed and the pyrolysis gases passed to a catalyst reactor containing different Ni-Al_2O_3 catalysts by Yang et al, [18]. They showed that the quality of the product carbon nanotubes was influenced by catalyst temperature. We have also reported [19] the importance of catalyst temperature in determining the quality of carbon nanotubes from pyrolysis-catalysis of low density polyethylene. Too high a temperature (900 °C) distorting the product carbon nanotubes. Further, the influence of metal promoters in the nickel catalyst also affect the yield and quality of carbon nanotubes, for example Fe and Co have been shown to promote carbon nanotube formation [20].

For the development of the process for the production of carbon nanotubes from waste plastics, using pyrolysis-catalysis, a route to recover the carbon nanotubes from the catalyst is required [20, 21]. The carbon nanotubes can become encapsulated and intermingled with the catalyst particles, making recovery of the carbon nanotubes difficult. Stainless steel mesh has been applied by many researchers in the production of CNTs from different feedstocks [22, 23, 24, 25, 26]. For example, Alves et al. [23] produced carbon nanotubes using a stainless steel type 304 alloy (Fe:Cr:Ni). It has also been reported that iron in the form of stainless steel promotes CNTs growth [24, 25]. Sano et al. [24] produced aligned multi-walled carbon nanotubes on the surface of stainless steel from phenol decomposition. The stainless steel mesh was activated by intensive oxidisation in air followed by reduction in H_2. Vander Wal and Hall [26] used activated type 304 stainless steel mesh as a catalyst to produce carbon nanotubes

from hydrocarbon gas mixtures such as C_2H_2/benzene or a CO/benzene mixture by chemical vapour deposition method.

However, there are few reports concerning the use of stainless steel mesh based catalysts for CNTs production from waste plastic. In this work, a Ni-based stainless steel mesh catalyst has been chosen to produce CNTs from the pyrolysis-catalysis of waste high density polyethylene using a two-stage reaction system. The temperature of the catalyst and the ratio of plastic sample to catalyst were also investigated.

2. Materials and Methods

2.1. Materials

High density polyethylene (HDPE), particle size ~2mm, was purchased from ACROS Organics UK. Stainless steel gauze was purchased from Alfa Aesar and was used as catalyst support for the nickel-stainless steel catalyst. The mesh was woven from 0.028 mm diameter stainless steel wire. The mesh was cut into squares (~ 4mm) and pre-treated by immersion into concentrated HNO_3 acid for 30 min, washed with de-ionized water, followed by drying at 100 °C for 3h and calcination at 800 °C for 3h with a heating rate of 10 °C min^{-1} in a static air atmosphere. For the loading of Ni on the pre-treated stainless steel mesh (SS), $NiCl_2$, ammonia solution and water were mixed and added to the mesh and dried in an oven at 90 °C for about 12 h. The produced stainless steel mesh loaded with nickel was water washed then dried at 105 °C. Calcination of the Ni-stainless steel precursor was carried out at 900 °C for 3 h. The prepared catalyst was characterised by SEM and XRD.

2.2. Pyrolysis-catalysis reactor

The pyrolysis-catalysis of the high density polyethylene was investigated using a two-stage fixed-bed reactor (Figure 1). The reactors were constructed of stainless steel with a diameter

of 2.2 cm and a height of 20 cm for the pyrolysis stage and 30 cm for catalysis stage and were heated by electrically heated furnaces with full monitoring and control for each stage. N_2 was used as the purge gas throughout the experiments at a fixed metered flow rate of 80 ml min^{-1}. The low rate of nitrogen will affect the residence time of the reactants over the catalyst and hence influence the formation of carbon on the catalyst. The HDPE sample was placed in the first stage pyrolysis reactor and pyrolysed at a heating rate of 40 °C min^{-1} to a final pyrolysis temperature of 500 °C. The second stage catalytic reactor was pre-heated to 800 °C and contained the nickel loaded stainless steel mesh catalyst. The total reaction time was 40 mins with an extra 20 mins gas collection time. The influence of catalyst temperature on the process was investigated at temperatures of 700, 800 and 900 °C and with a plastic to catalyst ratio of 2:1. In addition, a plastic to catalyst ratio of 4:1 was investigated at 900 °C catalyst temperature. Carbon was deposited on the nickel-stainless steel mesh catalyst during the pyrolysis-catalysis experiments. Product oils were collected in a dry-ice cooled condenser system and uncondensed gases passed to a Tedlar™ gas sample bag [22, 27]. The solid residue in the HDPE pyrolysis stage was measured by the weight difference of sample crucible before and after reaction. The carbon production was measured by the weight difference of reactor tube before and after reaction. The condensed liquid oil production was measured by the weight difference of the condensation system before and after reaction.

2.3. Analytical methods

The prepared nickel-loaded stainless steel catalysts were analysed by X-Ray Diffraction (XRD) using a SIEMENS D5000 instrument in the range of 10° ─ 70° using Cu Kα radiation at a wavelength of 0.1542. The gaseous products were analysed off-line with two Varian 3380 gas chromatographs (GC) [27]. One GC was used for H_2, CO, O_2 and N_2 and was fitted with a 2m long, 2mm diameter, 60-80mm mesh molecular sieve column and a thermal conductivity

detector. Within the GC was a second column which was 2m long, 2mm diameter containing molecular sieve material of 80-100mm mesh, which was connected to a thermal conductivity detector and was used for the quantitation of CO_2. The second GC used a 80-100 mm mesh HayeSep molecular sieve column and flame ionization detector for the analysis of $C_1 - C_4$ hydrocarbon gases.

The deposited carbons on the nickel-stainless steel mesh catalyst were removed from the mesh and were analysed by temperature programmed oxidation (TPO) using a Shimadzu thermogravimetric analyser (TGA) in order to understand the mass and type of deposited carbon. Scanning electron microscopy (SEM) using a Hitachi SU8230 SEM and also transmission electron microscopy (TEM) using a Tecnai TF20 were used to observe the characteristics of the deposited carbons. Raman analysis results were used to indicate the graphitic of carbon deposited on the Nickel-stainless steel mesh catalyst with a Renishaw Invisa Raman spectroscope. The system used a wavelength of 514 nm and the Raman shift wavelengths were between 1000 and 3200 cm^{-1}.

3. Results and discussion

3.1. Characteristics of the fresh catalyst

The freshly prepared nickel-loaded stainless steel catalyst was examined using scanning electron microscopy and example micrographs are shown in Figure 2. Figure 2(a) shows the low magnification image of the catalyst where the interlocking grid wires of the stainless steel mesh can be clearly seen. Figure 2(b) and 2(c) show higher magnification micrograms of the wire mesh surface showing a crystalline structure. Figure 3 shows an X-ray diffraction pattern of the freshly prepared nickel-loaded stainless steel catalyst indicating the presence of NiO, NiO/FeNi, FeNi and NiO peaks. During the pyrolysis of high density polyethylene, reducing

gases including hydrogen and carbon monoxide are produced which serve to reduce the catalyst and produce nickel and nickel-iron phases.

3.2. Product yield

The product yield and gas composition resulting from the pyrolysis-catalysis of high density polyethylene (HDPE) in the presence of the nickel-stainless steel catalyst in relation to catalyst temperature and also plastic to catalyst ratio are shown in Table 1. The results show that there was little influence of catalyst temperature on the yield of gas at each plastic to catalyst ratio, however, the liquid product yield showed a significant reduction from 17.00 wt.% at 700 °C to 10.50 wt.% at 900 °C catalyst temperature. Importantly, the carbon deposited on the nickel loaded stainless steel mesh catalyst showed an increase in yield from 32.50 wt.% to 38.00 wt.%. The residue yield in Table 1 refers to the mass of pyrolysis char in the pyrolysis reactor after the experiments, which was negligible at ~0.5 wt.%. Table 1 also shows the influence of increasing the plastic to catalyst ratio from 2:1 to 4:1 at a nickel-stainless steel mesh catalyst temperature of 900 °C. The results show that increasing the plastic to catalyst ratio increased the gas yield from ~51 wt.% to 62.62 wt.%, and the carbon deposition was reduced from 38.00 to 25.75 wt.%. The liquid yield was largely unaffected by change in plastic to catalyst ratio.

Table 1 also shows the composition of the product gases in relation to the nickel-stainless steel mesh catalyst temperature and plastic to catalyst ratio. The main gases produced during the pyrolysis-catalysis of the HDPE were hydrogen, carbon monoxide, methane and C_2 – C_4 hydrocarbons. The gas product therefore has a significant calorific value which could be used as process fuel for the system. The increase of catalysis temperature from 700 to 900 °C resulted in an increase of the CO concentration from 0.78 to 3.02 vol.% and the concentration of hydrogen was the highest at 51.03 vol.%, when the catalyst temperature was at 900 °C. The concentration of hydrocarbon gases (C_2-C_4) decreased from 26.69 to 12.92 wt. % as the

catalysis temperature was increased from 700 to 900 °C. The decomposition of plastics to form gas products and solid carbon have been described via the following reactions [28]:

Thermal cracking: $pC_nH_x \rightarrow qC_mH_y + rH$ (1)

Carbon formation: $C_nH_x \rightarrow nC + x/2\ H_2$ (2)

During the pyrolysis-catalysis of plastics, the polyalkene HDPE plastic was initially degraded into smaller organic compounds, then these compounds were dehydrogenated to produce carbon products and gaseous products [19]. The product oils and gases which are generated from the pyrolysis of the HDPE and which pass over the stainless steel mesh catalyst have been analysed before and shown to be largely aliphatic in composition [29-31]. The gases produced are mainly methane, ethane, ethene, propane, propene, butane and butene, with lower concentrations of hydrogen and carbon monoxide [31]. Depending on the plastic pyrolysis conditions and the condensation temperature and system design, the product oil can represent an oil or wax-like product. The waxes when analysed by high temperature gas chromatography have been shown to consist of alkane, alkene and alkadiene hydrocarbons in the range up to C_{60} and the oils typically have a hydrocarbon range up to C_{40} with a peak at C_{20} [29]. However, much higher molecular weight hydrocarbons can be detected using size exclusion chromatography [30, 31]. Therefore, the thermal degradation of the HDPE via a random scission mechanism [29] might be expected to produce a wide range of aliphatic hydrocarbon gases, oils and waxes and polymer fragments from light gases up to heavy molecular weight species which then pass over the stainless steel mesh catalyst, cracking the pyrolysis gases and also depositing carbon nanotubes.

It is suggested that a higher gasification temperature promoted the secondary reactions in the polyethylene pyrolysis-catalysis process resulting in the enhancement of hydrogen and carbon monoxide production [29 (32)]. When the sample to catalyst ratio was increased from 2:1 to 4:1 at 900 °C catalyst temperature, H_2 concentration decreased from 51.03 to 35.59 vol.%,

CO concentration decreased from 3.02 to 2.23 vol. % and hydrocarbon gases concentration increased from 12.92 to 23.13 vol.%.

3.3. Carbon production and characterization

The carbon deposited on the nickel loaded catalyst was collected by physical separation from the mesh catalyst and characterised by several techniques. Thermogravimetric analysis (TGA) using temperature programmed oxidation (TPO) of the collected carbon deposits was carried out and the results are shown Figure 4 [33]. TGA-TPO characterisation enables the oxidation of the carbon in an air atmosphere in relation to a temperature controlled fixed heating rate. The different type of carbon deposit oxidise at different temperatures, for example disordered/amorphous carbons oxidise at lower temperatures than graphitic, filamentous type carbons [14]. It was assumed the weight loss which occurred before 600 °C oxidation temperature was assigned as the oxidation of amorphous type carbon and the weight loss that occurred after 600 °C was assigned as filamentous carbon [18, 27, 32]. Based on the differentiation of the two types of carbon deposited on the nickel-stainless steel mesh catalysts using the data from the TGA-TPO (Figure 4), the mass of filamentous and amorphous carbons were calculated and the results are shown in Figure 5. The weight of filamentous carbon increased from 316.35 mg g^{-1} plastic at 700 °C catalyst temperature to 374.06 mg g^{-1} at 900 °C catalyst temperature. It is suggested that more heavy hydrocarbons were decomposed into light hydrocarbons when the catalysis temperature was increased; these produced light hydrocarbons which are suggested to provide more carbon sources for the formation of filamentous carbons. It is consistent with the changes of C_2-C_4 gaseous productions shown in Table 1, when the catalysis temperature was increased from 700 to 900 °C, C_2-C_4 hydrocarbon concentrations decreased from 26.69 to 12.92 vol.%.

Fang et al. [33] reported that the oxidation peak of filamentous carbons with smaller diameters occurred at lower temperatures during TGA-TPO analysis compared with oxidation of filamentous carbons with larger diameters which occurred at higher oxidation temperatures. In addition, Li et al. [34] differentiated between the TGA-TPO characterisation of single walled carbon nanotubes compared with multi-walled carbon nanotubes, where the single-walled CNTs were oxidised at lower oxidation temperatures compared to multi-walled CNTs which oxidised at higher temperatures. They suggested that the oxidation of MWCNTs occurred at higher temperature because of strong interaction between graphite layers in the MWCNTs, which stabilised the structure of MWCNTs indicating higher thermal stability compared with single-wall CNTs. Consequently, the TGA-TPO data might indicate that the carbon oxidation at higher temperature corresponds to filamentous carbons, including multi-walled carbon nanotubes.

Increasing the plastic to catalyst ratio from 2:1 to 4:1 resulted in a decrease in filamentous carbon deposition from 374.06 to 247.03 mg g^{-1} plastic. Li et al. [34] reported that an increased sample to catalyst ratio enhanced the carbon dissolving rate into the metal particles of the catalyst compared with the rates of carbon diffusing and precipitating, thus the formation of filamentous carbons were prohibited [35].

Figure 6(a), 6(b) and 6(c) shows the SEM micrographs of the carbons formed on the reacted nickel-stainless steel mesh catalyst. It is clear that the diameters of filamentous carbons formed at catalysis temperature at 700 °C are smaller than the filamentous carbons formed at higher catalyst temperature when the sample to catalyst ratio was 2:1. Figure 7(a) and 7(b) (TEM analysis) confirm the presence of MWCNTs as the type of carbon deposited on the nickel-stainless steel mesh catalyst. The carbon nanotubes were typically 10 ─ 20 nm diameter and more than 1 μm in length. In addition, there were some solid carbon fibres in addition to the MWCNTs observed with TEM analysis. Estimation of the amount of MWCNTs compared

to solid fibre filamentous carbons and amorphous carbons using TEM, suggested that approximately 40% were MWCNTs. Kumar and Ando [36] reported an increase of diameters of CNTs with the increase of reaction temperature with a chemical vapour deposition process using pure hydrocarbon as feedstock. However, Gong et al. [37] pointed out the mechanism of CNTs growth from polyalkene plastics is different from using pure hydrocarbon gas, because of complicated products which are produced from such polymers including gas, liquid and semi-liquid products. The authors proposed that there were synergistic reactions between light hydrocarbons and aromatic compounds.

Raman spectroscopy is a technique used to characterize the structures of carbon materials, including the amorphous and/or graphitic carbons [33, 38, 39, 40, 41]. As shown in Fig. 8, the Raman spectra in the wavelength range of 1000 to 2750 cm^{-1} are presented to compare the carbons produced at different catalysis temperature when the sample to catalyst ratio was 2:1. The D band centred at 1300 cm^{-1} suggests an amorphous or disordered carbon structure. The G band centred at 1550 cm^{-1} indicates filamentous or ordered carbons which correspond to the tangential vibrations of the graphite carbons. The G' band in the Raman shift at a wavelength around 2700 cm^{-1} indicates the purity of carbons [21, 38]. The graphitization of carbon production can be evaluated by the I_D/I_G ratio which is the intensity of the D band normalized to the G band. The I_D/I_G ratios of the carbons produced at different catalysis temperatures are displayed in Figure 8 and are 1.18, 1.25 and 1.53 for the carbons produced at catalysis temperatures of 700, 800 and 900 ^oC respectively. The ratio indicating that disordered carbons are present in addition to graphitic carbons. The I_D/I_G ratios of commercial multi-walled carbon nanotubes produce typical ratios of between 0.63-1.5 [12]. The results show that the degree of graphitization of the carbons produced from HDPE by pyrolysis-catalysis with the nickel-stainless steel mesh catalyst in this work are within the range of commercial carbon nanotubes. The $I_{G'}/I_G$ ratio obtained from Raman spectroscopy can be used to estimate the

purity of carbon where the presence of the G' band indicates defects in the graphitic chrystallinity of the carbon [38, 40]. When a catalysis temperature of 800 °C was used the $I_{G'}/I_G$ ratio was the lowest at 0.48 indicating the carbons are the most graphitic compared with the carbons produced at 700 and 900 °C.

Overall, this work has shown that significant yields of graphitic, long length, carbon nanotubes can be produced from the two-stage pyrolysis-catalysis of high density polyethylene. The carbon nanotubes have relatively small diameters (10 ─ 20 nm) and are several microns in length. The use of the nickel-loaded stainless steel mesh enables the carbon nanotubes which are deposited on the catalyst during the reaction to be easily physically removed from the mesh, which aids catalyst re-use and carbon nanotube utilisation.

4. Conclusions

In this study, different catalysis temperatures (700, 800 and 900 ºC), and different sample to catalyst ratios (2:1 and 4:1) were investigated for the pyrolysis-catalysis of high density polyethylene for the production of high value carbon products, including carbon nanotubes. The catalysis consisted of a stainless steel mesh which had been loaded with nickel to produce a nickel-stainless steel catalyst. Carbon was deposited onto the mesh catalyst during the process of pyrolysis-catalysis of the high density polyethylene. The influence of catalyst temperature was to produce increasing deposits of carbon on the mesh catalyst from 32.5 wt.% at 700 °C catalyst temperature rising to 38.0 wt.% at 900 °C. Using a higher plastic to catalyst feed ratio resulted in a reduction in catalyst carbon deposition at 900 °C. The carbon was easily removable from the stainless steel mesh catalyst and was characterised by a number of techniques. Electron microscopy (SEM and TEM) examination of the carbon revealed that the carbon consisted of mainly filamentous carbons, which consisted of a high proportion (~40%) multi-walled carbon nanotubes. The carbons were also analysed using Raman spectroscopy

which suggested that carbon nanotube quality was influenced by process conditions. Optimal conditions for the production of high yields of high carbon nanotubes was 800 °C nickel-stainless steel mesh catalyst temperature and plastic to catalyst ratio of 1:2, where yields were more than 0.3 g filamentous/carbon nanotube type carbons for each gram of plastic feedstock.

Acknowledgement

This project has received funding from the European Union's Horizon 2020 research and innovation programme under the Marie Sklodowski-Curie grant agreement No. 643322 (FLEXI-PYROCAT).

Disclosure Statement

The authors have no conflict of interest to declare

References:

[1] Liang W, Bockrath M, Bozovic D, Hafner JH, Tinkham M, Park H. Fabry-Perot interference in a nanotube electron waveguide. Nature. 2001;411:665-9.

[2] Yao HB, Fang HY, Tan ZH, Wu LH, Yu SH. Biologically inspired, strong, transparent, and functional layered organic–inorganic hybrid films. Angew Chem. 2010;122:2186-91.

[3] Baughman RH, Zakhidov AA, de Heer WA. Carbon nanotubes--the route toward applications. Science. 2002;297:787-92.

[4] Dai H. Carbon nanotubes: opportunities and challenges. Surf Sci. 2002;500:218-41.

[5] Das N, Dalai A, Soltan Mohammadzadeh JS, Adjaye J. The effect of feedstock and process conditions on the synthesis of high purity CNTs from aromatic hydrocarbons. Carbon. 2006;44:2236-45.

[6] Joselevich E, Dai H, Liu J, Hata K, Windle AH. Carbon nanotube synthesis and organization. Carbon nanotubes: Advanced Topics in the Synthesis, Structure, Properties and Applications: Springer; 2007.

[7] Kong J, Cassell AM, Dai H. Chemical vapor deposition of methane for single-walled carbon nanotubes. Chem Phys Lett. 1998;292:567-74.

[8] Wei Y, Eres G, Merkulov V, Lowndes D. Effect of catalyst film thickness on carbon nanotube growth by selective area chemical vapor deposition. Appl Phys Lett. 2001;78:1394-6.

[9] Kumar M, Ando Y. Carbon nanotube synthesis and growth mechanism. In: Yellampalli S, editor. Nanotechnology and nanomaterials; Carbon nanotubes-Synthesis, characterisation, application: INTECH Open Access Publisher; 2011.

[10] Chai S-P, Zein SHS, Mohamed AR. Synthesizing carbon nanotubes and carbon nanofibers over supported-nickel oxide catalysts via catalytic decomposition of methane. Diam Relat Mater. 2007;16:1656-64.

[11] Jung M, Eun KY, Baik Y-J, Lee K-R, Shin J-K, Kim S-T. Effect of NH_3 environmental gas on the growth of aligned carbon nanotube in catalystically pyrolizing C_2H_2. Thin Solid Films. 2001;398:150-5.

[12] Wu C, Wang Z, Wang L, Williams PT, Huang J. Sustainable processing of waste plastics to produce high yield hydrogen-rich synthesis gas and high quality carbon nanotubes. RSC Advs. 2012;2:4045-7.

[13] Bazargan A, McKay G. A review–Synthesis of carbon nanotubes from plastic wastes. Chem Eng J. 2012;195:377-91.

[14] Kukovitskii EF, Chernozatonskii LA, L'Vov SG, Mel'nik NN. Carbon nanotubes of polyethylene. Chem Phys Lett. 1997;266:323-8.

[15] Yen Y-w, Huang M-D, Lin F-J. Synthesize carbon nanotubes by a novel method using chemical vapor deposition-fluidized bed reactor from solid-stated polymers. Diam Relat Mater. 2008;17:567-70.

[16] Liu J, Jiang Z, Yu H, Tang T. Catalytic pyrolysis of polypropylene to synthesize carbon nanotubes and hydrogen through a two-stage process. Polym Degrad Stabil. 2011;96:1711-9.

[17] Wu C, Nahil MA, Miskolczi N, Huang J, Williams PT. Processing real-world waste plastics by pyrolysis-reforming for hydrogen and high-value carbon nanotubes. Environ Sci Technol. 2013;48:819-26.

[18] Yang R-X, Chuang K-H, Wey M-Y. Effects of Nickel Species on Ni/Al_2O_3 Catalysts in carbon nanotube and hydrogen production by waste plastic gasification: Bench- and pilot-scale tests. Energ Fuel. 2015;29:8178-87.

[19] Acomb JC, Wu C, Williams PT. Effect of growth temperature and feedstock:catalyst ratio on the production of carbon nanotubes and hydrogen from the pyrolysis of waste plastics. J Anal Appl Pyrolysis. 2015;113:231-8.

[20] Acomb JC, Wu C, Williams PT. The use of different metal catalysts for the simultaneous production of carbon nanotubes and hydrogen from pyrolysis of plastic feedstocks. Appl. Catal B-Environ. 2016;180:497-510.

[21] Wu C, Wang Z, Williams PT, Huang J. Renewable hydrogen and carbon nanotubes from biodiesel waste glycerol. Sci Report. 2013;3.

[22] Wu C, Huang J, Williams PT. Carbon nanotubes and hydrogen production from the reforming of toluene. Int J Hydrogen Energ. 2013;38:8790-7.

[23] Alves JO, Levendis YA, Tenório JAS. Synthesis of nanomaterials from unserviceable tires. Carbon. 2012;85:82.2.

[24] Sano N, Hori Y, Yamamoto S, Tamon H. A simple oxidation–reduction process for the activation of a stainless steel surface to synthesize multi-walled carbon nanotubes and its application to phenol degradation in water. Carbon. 2012;50:115-22.

[25] Amadou J, Begin D, Nguyen P, Tessonnier JP, Dintzer T, Vanhaecke E, Ledoux MJ, Pham-Huu C. Synthesis of a carbon nanotube monolith with controlled macroscopic shape. Carbon. 2006;44:2587-9.

[26] Vander Wal RL, Hall LJ. Carbon nanotube synthesis upon stainless steel meshes. Carbon. 2003;41:659-72.

[27] Zhang Y, Wu C, Nahil MA, Williams P. Pyrolysis–catalytic reforming/gasification of waste tires for production of carbon nanotubes and hydrogen. Energ Fuel. 2015;29:3328-34.

[28] Kaewpengkrow P, Atong D, Sricharoenchaikul V. Pyrolysis and gasification of landfilled plastic wastes with Ni− Mg− La/Al2O3 catalyst. Environ Technol. 2012;33:2489-95.

[29] Schiers J, Kaminsky W, Feedstock Recycling Recycling and Pyrolysis of Waste Plastics. John Wiley & Sons Ltd, Chichester; 2006

[30] Williams PT, Williams EA, Interaction of plastics in mixed plastics pyrolysis'. Energ Fuel. 1999;13:188-196.

[31] Williams EA Williams PT, The pyrolysis of individual plastics and a plastic mixture in a fixed bed reactor. J Chem Technol Biotechnol. 1997:70:9-20.

[32] Wu C, Williams PT. Hydrogen production from the pyrolysis−gasification of polypropylene: Influence of steam flow rate, carrier gas flow rate and gasification temperature. Energ Fuel. 2009;23:5055-61.

[33] Fang W, Pirez C, Capron M, Paul S, Raja T, Dhepe PL, Dumeignil F, Jalowiecki-Duhamel L. Ce-Ni mixed oxide as efficient catalyst for H_2 production and nanofibrous carbon material from ethanol in the presence of water. RSC Advs. 2012;2:9626-34.

[34] Li Q, Yan H, Zhang J, Liu Z. Effect of hydrocarbons precursors on the formation of carbon nanotubes in chemical vapor deposition. Carbon. 2004;42:829-35.

[35] Li W, Wen J, Ren Z. Effect of temperature on growth and structure of carbon nanotubes by chemical vapor deposition. Appl Phys A. 2002;74:397-402.

[36] Kumar M, Ando Y. Chemical vapor deposition of carbon nanotubes: a review on growth mechanism and mass production. J Nanosci Nanotech. 2010;10:3739-58.

[37] Gong J, Liu J, Wan D, Chen X, Wen X, Mijowska E, Jiang Z, Wang Y, Tang T. Catalytic carbonization of polypropylene by the combined catalysis of activated carbon with Ni2O3 into carbon nanotubes and its mechanism. Appl Catal A-Gen. 2012;449:112-20.

[38] Dresselhaus MS, Dresselhaus G, Jorio A, Souza Filho AG, Saito R. Raman spectroscopy on isolated single wall carbon nanotubes. Carbon. 2002;40:2043-61.

[39] Carrero A, Calles JA, Vizcaíno AJ. Effect of Mg and Ca addition on coke deposition over Cu–Ni/SiO2 catalysts for ethanol steam reforming. Chem Eng J. 2010;163:395-402.

[40] DiLeo RA, Landi BJ, Raffaelle RP. Purity assessment of multiwalled carbon nanotubes by Raman spectroscopy. J Appl Phys. 2007;101:064307.

[41] Ferrari AC, Robertson J. Raman spectroscopy of amorphous, nanostructured, diamond–like carbon, and nanodiamond. Phil Trans Roy Soc -A: Math Phys Eng Sci. 2004;362:2477-512.

Table 1 Mass balance and gas concentrations for the pyrolysis-catalysis of high density polyethylene (HDPE) in relation to catalyst temperature and different plastic to catalyst ratio.

HDPE weight (g)	2	2	2	4
Temperature (˚C)	700	800	900	900
Sample to catalyst ratio	2:1	2:1	2:1	4:1
Gas yield (wt. %)	50.44	51.99	51.13	62.62
Liquid yield (wt. %)	17.00	14.00	10.50	9.75
Residue yield (wt. %)	0.50	0.50	0.50	0.50
Carbon yield (wt. %)	32.50	34.00	38.00	25.75
Mass balance (wt. %)	100.44	100.49	100.13	98.87
Gas concentration (Vol. %)				
CO	0.78	1.82	3.02	2.23
H_2	50.51	44.95	51.03	35.59
O_2	0.28	0.43	0.62	0.85
CO_2	0.26	0.33	0.33	0.21
CH_4	21.48	32.57	32.08	37.99
C_2-C_4	26.69	19.90	12.92	23.13

FIGURE CAPTIONS

Figure 1. Schematic diagram of the two stage fixed bed pyrolysis-catalytic reactor system

Figure 2. Scanning electron micrograph of the prepared nickel-loaded stainless steel mesh catalyst

Figure 3. X-ray diffraction analysis of the prepared nickel-loaded stainless steel mesh catalyst

Figure 4. TGA-TPO and DTG-TPO analysis of the deposited carbon in relation to catalyst temperature and different plastic to catalyst ratio.

Figure 5. Proportions of disordered carbon and filamentous carbon produced from HDPE by pyrolysis-catalysis with the nickel-stainless steel mesh catalyst

Figure 6. SEM analyses of carbon deposited on the wire mesh catalyst for the pyrolysis-catalysis of waste high density polyethylene in relation to catalyst temperature.

Figure 7. TEM analyses of carbon deposited on the wire mesh catalyst for the pyrolysis-catalysis of waste high density polyethylene at different catalyst temperatures.

Figure 8. Raman analyses of carbon deposited on the wire mesh catalyst for the pyrolysis-catalysis of waste high density polyethylene in relation to temperature.

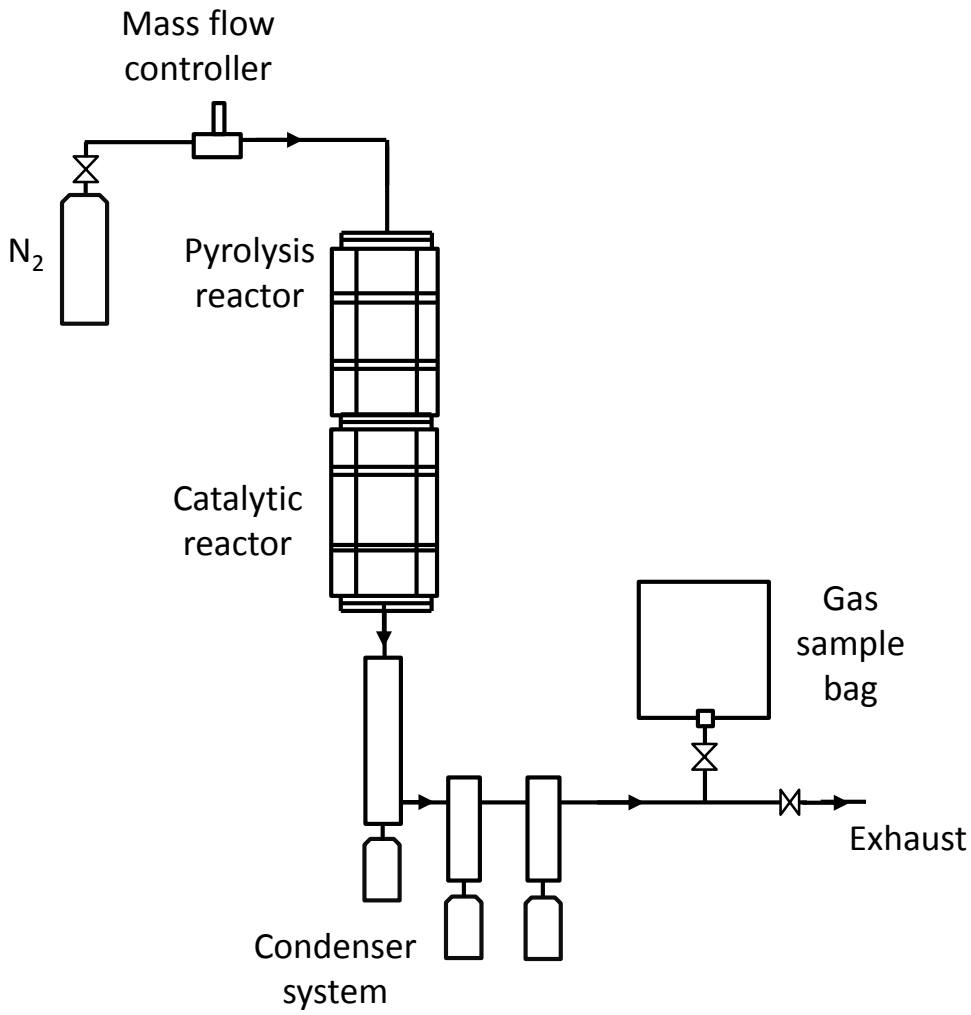
Mass flow
controller
N_2
Pyrolysis
reactor
Catalytic
reactor
Gas
sample
bag
Exhaust
Condenser
system

Figure 1.

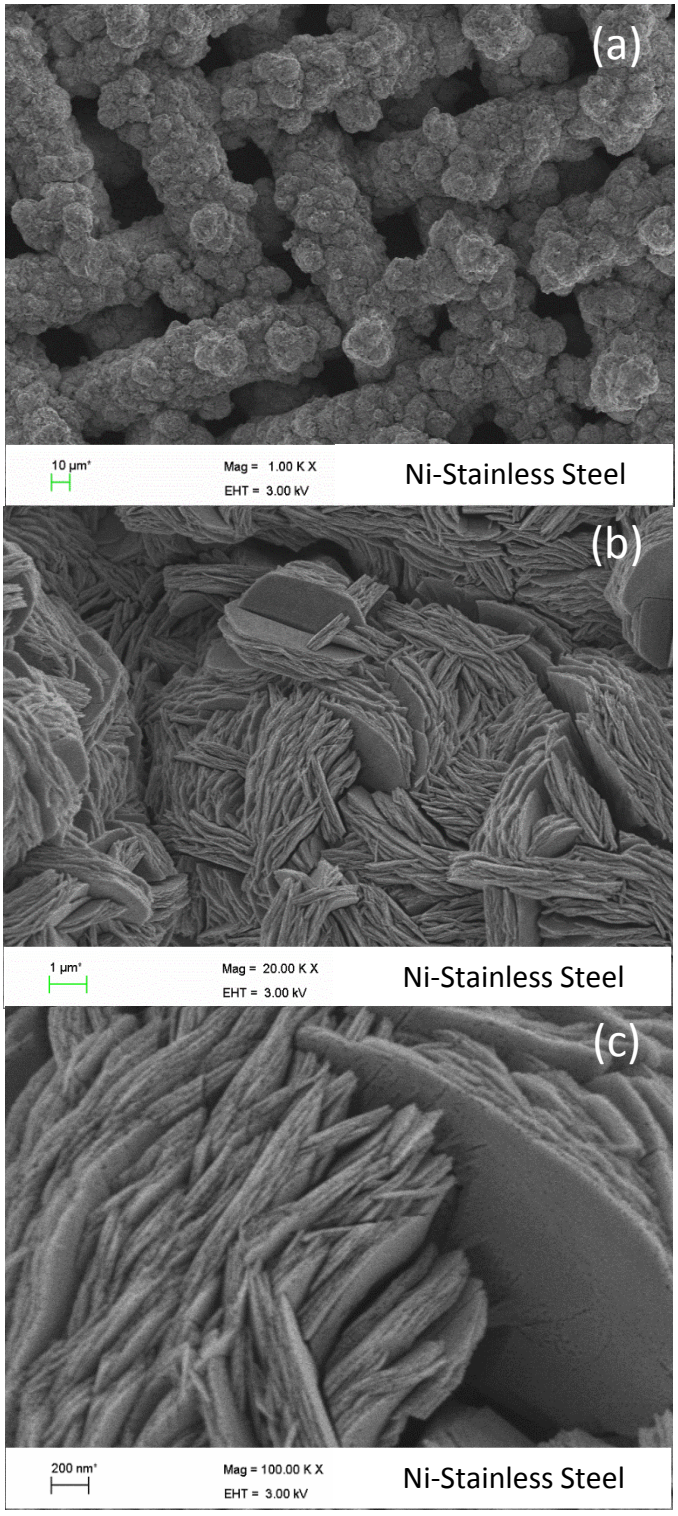
(a)
10 µm*
Mag = 1.00 K X
EHT = 3.00 kV
Ni-Stainless Steel
(b)
1 µm*
Mag = 20.00 K X
EHT = 3.00 kV
Ni-Stainless Steel
(c)
200 nm*
Mag = 100.00 K X
EHT = 3.00 kV
Ni-Stainless Steel

Figure 2.

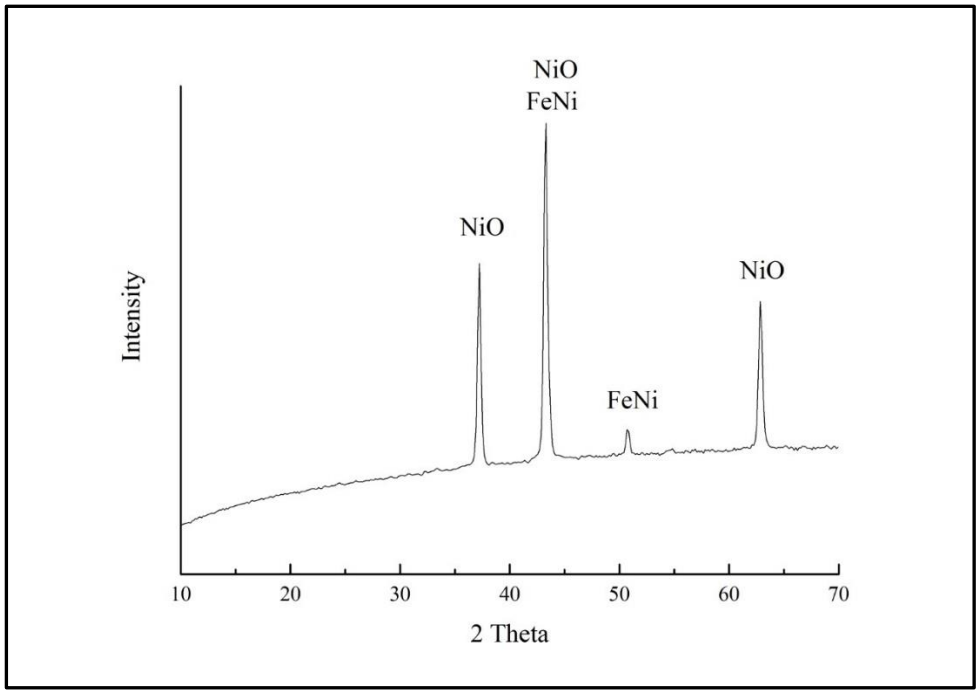

Figure 3.

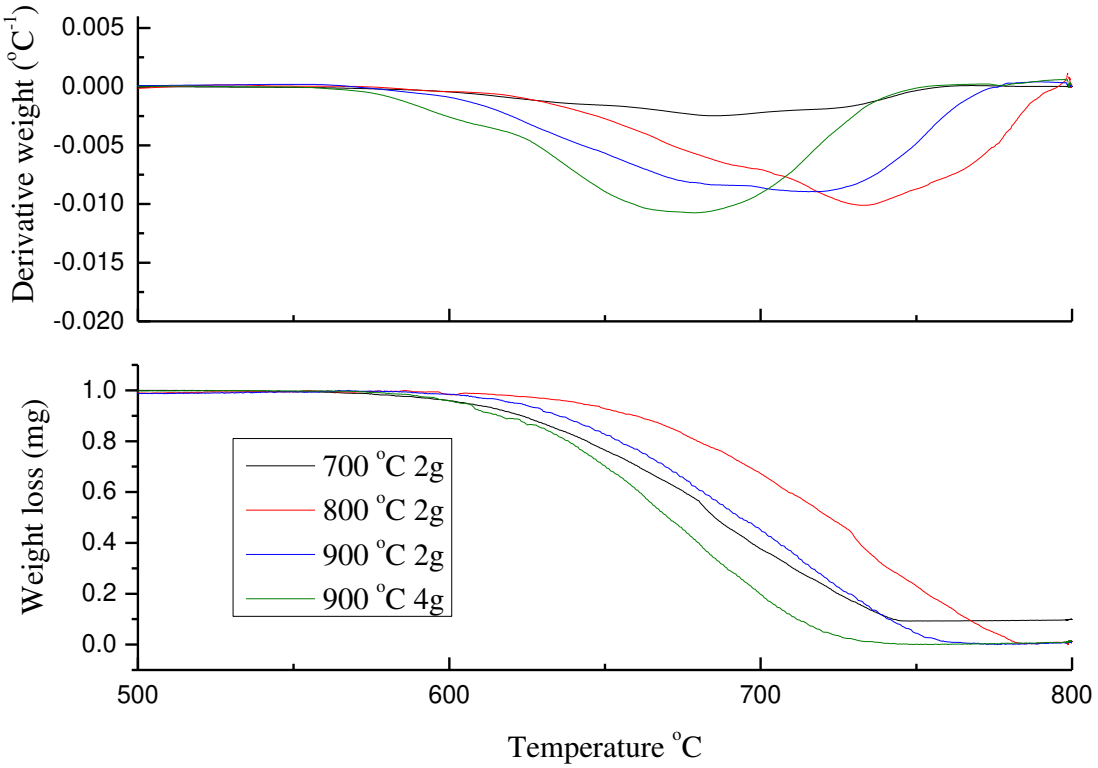
Derivative weight (°C-1)
0.005
0.000
-0.005
-0.010
-0.015
-0.020
Weight loss (mg)
1.0
0.8
0.6
0.4
0.2
0.0
700 °C 2g
800 °C 2g
900 °C 2g
900 °C 4g
500
600
700
800
Temperature °C

Figure 4.

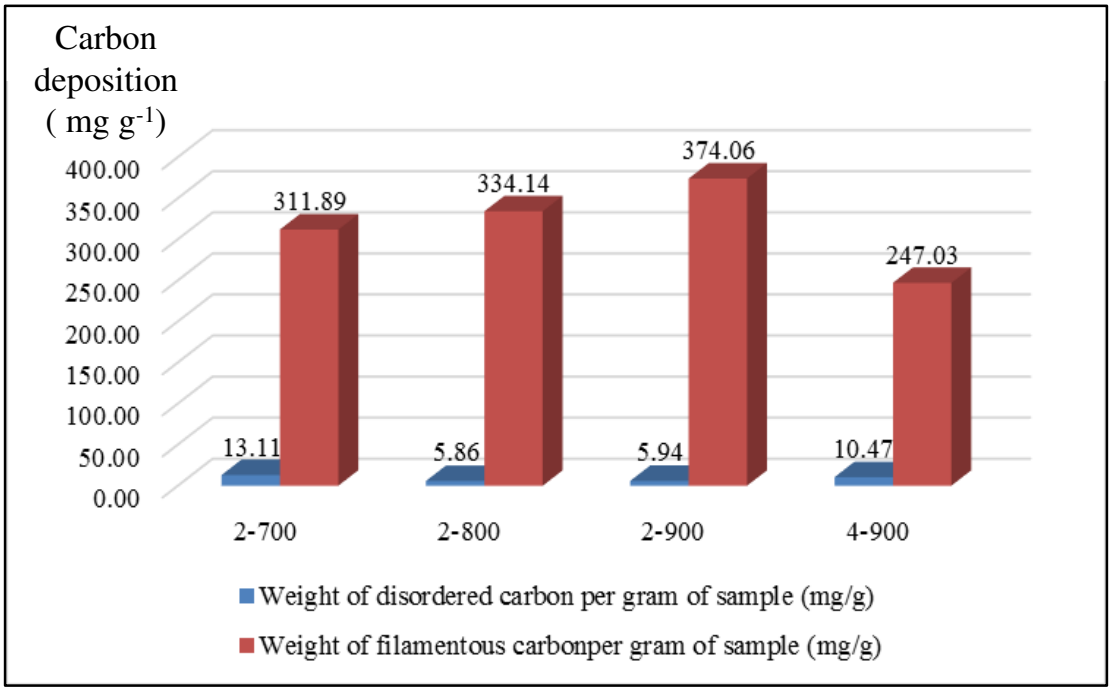
Carbon deposition (mg g-1)
400.00
350.00
300.00
250.00
200.00
150.00
100.00
50.00
0.00
311.89
334.14
374.06
247.03
13.11
5.86
5.94
10.47
2-700
2-800
2-900
4-900
Weight of disordered carbon per gram of sample (mg/g)
Weight of filamentous carbonper gram of sample (mg/g)

Figure 5.

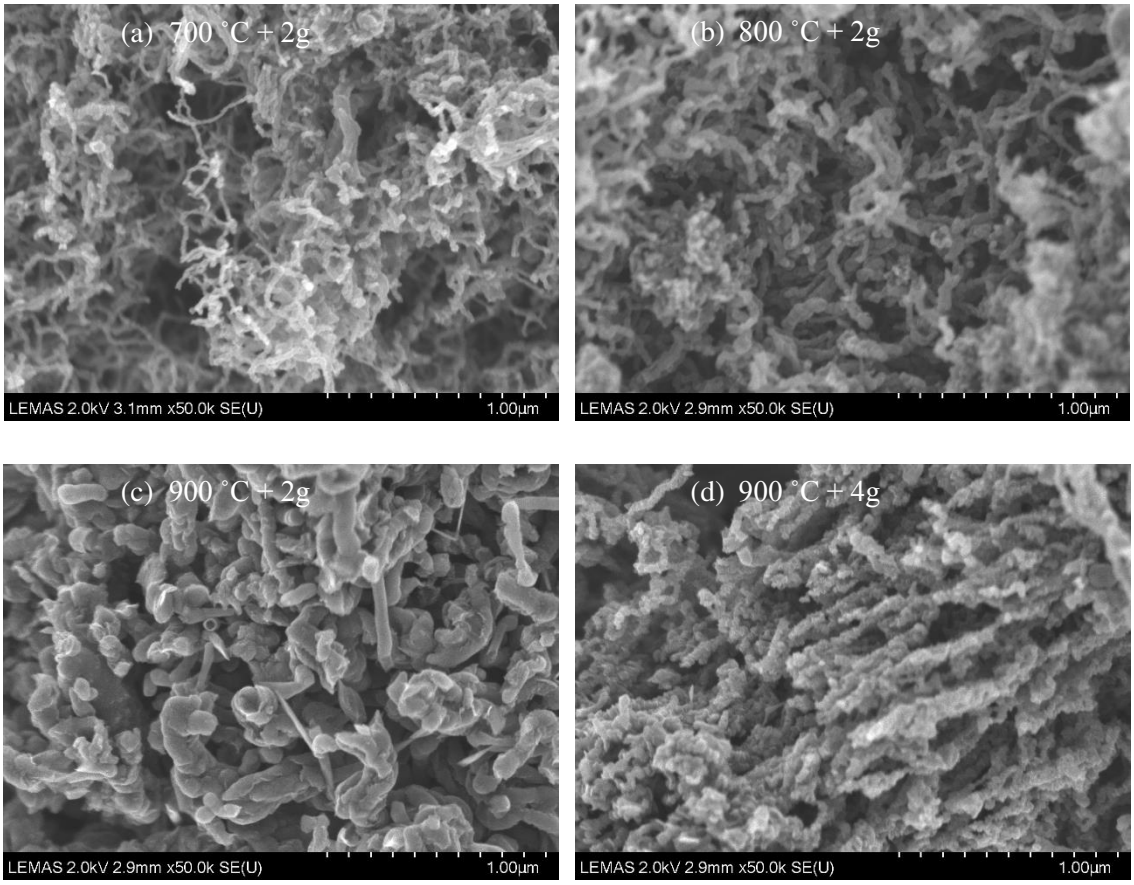
(a) 700 ˚C + 2g
LEMAS 2.0kV 3.1mm x50.0k SE(U)
1.00μm
(b) 800 ˚C + 2g
LEMAS 2.0kV 2.9mm x50.0k SE(U)
1.00μm
(c) 900 ˚C + 2g
LEMAS 2.0kV 2.9mm x50.0k SE(U)
1.00μm
(d) 900 ˚C + 4g
LEMAS 2.0kV 2.9mm x50.0k SE(U)
1.00μm

Figure 6.

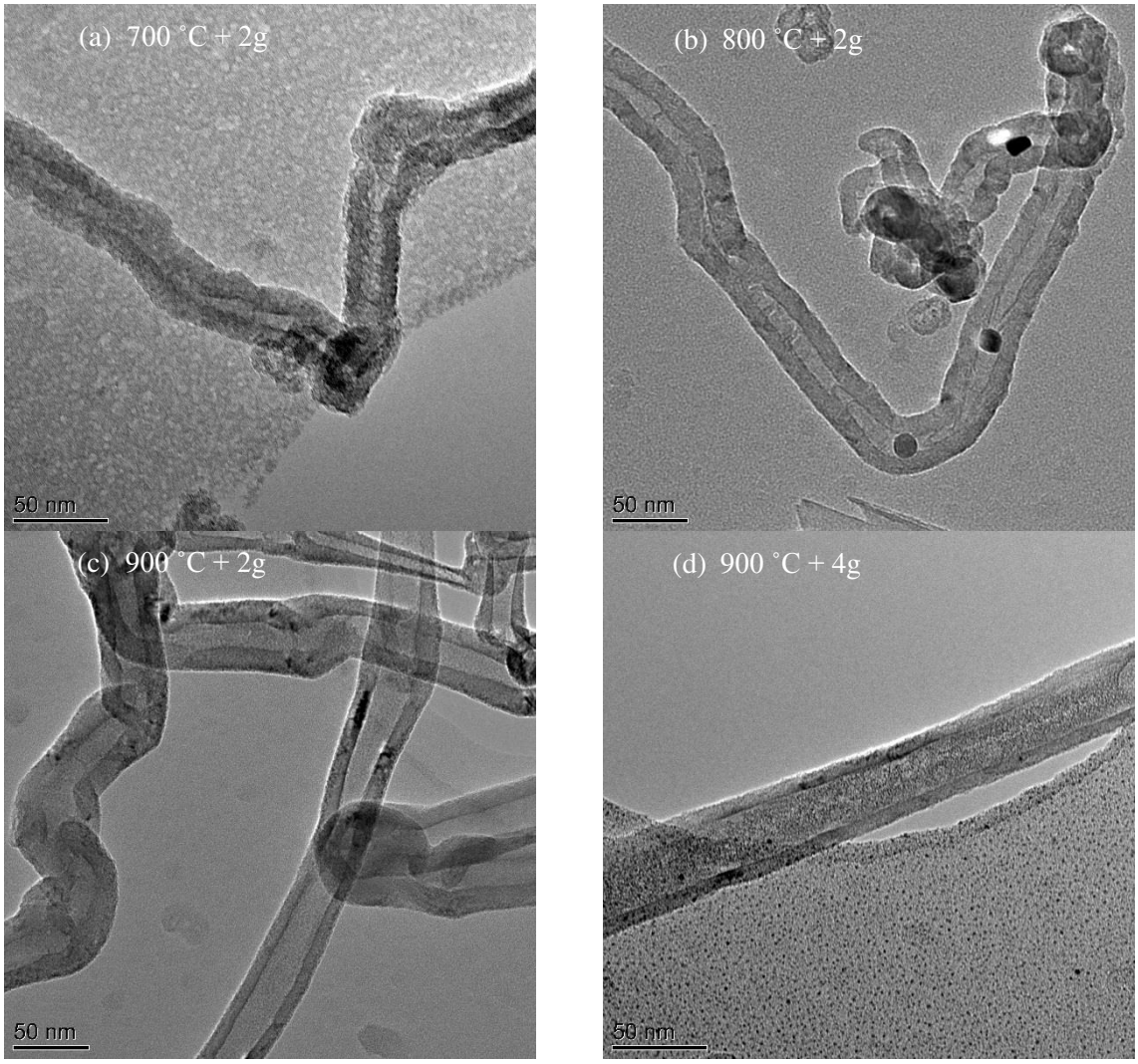

Figure 7.

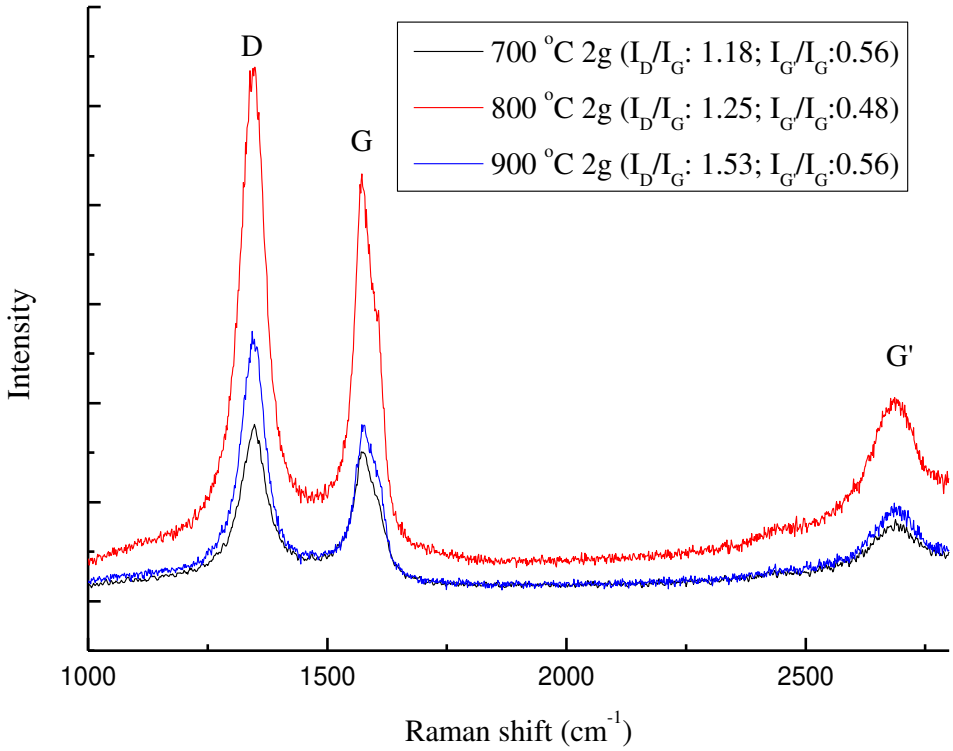
D
G
G'
700 °C 2g (I_D/I_G: 1.18; I_G/I_G:0.56)
800 °C 2g (I_D/I_G: 1.25; I_G/I_G:0.48)
900 °C 2g (I_D/I_G: 1.53; I_G/I_G:0.56)
Intensity
1000
1500
2000
2500
Raman shift (cm-1)

Figure 8.